



Probing the pH sensitivity of R-phycoerythrin: Investigations of active conformational and functional variation

Lu-Ning Liu¹, Hai-Nan Su¹, Shi-Gan Yan, Si-Mi Shao, Bin-Bin Xie, Xiu-Lan Chen, Xi-Ying Zhang, Bai-Cheng Zhou, Yu-Zhong Zhang^{*}

State Key Lab of Microbial Technology, Marine Biotechnology Research Center, Shandong University, Jinan 250100, PR China

ARTICLE INFO

Article history:

Received 20 November 2008

Received in revised form 15 February 2009

Accepted 17 February 2009

Available online 3 March 2009

Keywords:

Phycoerythrin

Stability

Tertiary structure

Spectra

Protein folding

ABSTRACT

Crystal structures of phycobiliproteins have provided valuable information regarding the conformations and amino acid organizations of peptides and chromophores, and enable us to investigate their structural and functional relationships with respect to environmental variations. In this work, we explored the pH-induced conformational and functional dynamics of R-phycoerythrin (R-PE) by means of absorption, fluorescence and circular dichroism spectra, together with analysis of its crystal structure. R-PE presents stronger functional stability in the pH range of 3.5–10 compared to the structural stability. Beyond this range, pronounced functional and structural changes occur. Crystal structure analysis shows that the tertiary structure of R-PE is fixed by several key anchoring points of the protein. With this specific association, the fundamental structure of R-PE is stabilized to present physiological spectroscopic properties, while local variations in protein peptides are also allowed in response to environmental disturbances. The functional stability and relative structural sensitivity of R-PE allow environmental adaptation.

© 2009 Elsevier B.V. All rights reserved.

1. Introduction

Phycobiliproteins (PBPs) are water-soluble light-harvesting proteins in cyanobacteria, red algae and cryptophytes [1–4]. With the assistance of linker polypeptides, these proteins are assembled in cyanobacteria and red algae into the external light-harvesting antennae complexes, termed phycobilisomes (PBsomes), attaching to the stromal surface of thylakoid membranes and harvesting light energy for the photosynthetic reaction centers embedded in the thylakoid membrane [5–7].

PBPs are strong fluorescing, which is ascribed to the presence of open-chain tetrapyrrole chromophores covalently attached to specific cysteine residues of apoprotein by thioether bonds. On the basis of different spectroscopic properties and bilin types, PBPs are commonly divided into four classes: phycoerythrins (PEs, λ_{\max} = 540–570 nm), phycocyanins (PCs, λ_{\max} = 610–620 nm), allophycocyanins (APCs, λ_{\max} = 650–655 nm) and phycoerythrocyanins (PECs) [8,9]. The native globin structure frame of PBPs, formed by proper folding of the apoproteins, provides the chromophores with a stable local environment and facilitates highly efficient dipole–dipole resonance energy

transfer between closely coupled chromophores. Chromophores with similar chemical structures can present different spectral characteristics due to variations in the local micro-environment, such as changes in the orientation of chromophores and the distance between neighboring chromophores [10]. Therefore, chromophore–protein complexes can be applied for the study of structural dynamics, as considerable information can be provided during the folding/unfolding process by the chromophore [11–13], such as C-phycocyanin, one kind of PBP-carrying phycocyanobilin [13]. Compared to the phycocyanobilin-containing proteins, there is little work on phycoerythrobin (PEB) and phycourobilin (PUB) containing biliproteins.

The large amount of available X-ray crystallography data of PBPs in cyanobacteria and red algae reveals that they share highly similar protein conformations [6,8]. So far, only one X-ray structure of a linker polypeptide has been resolved in APC trimer [14]. The R-phycoerythrins (R-PEs) of *Polysiphonia* (*P. urceolata*), with the heteropolymer state of ($\alpha\beta$)₆ γ , contain phycoerythrobin (PEB) and phycourobilin (PUB). These proteins provide photosynthetic species with a broader and blue-shifted absorption ability. The crystal structure of R-PE from *P. urceolata* at 2.8 Å resolution has been solved [15]. It shows: the α subunit of R-PE has 2 PEB at α 84 and α 140; the β subunit has 2 PEB at β 84 and β 155 and 1 PUB at β 50/61; the γ subunit has 3 PUB and 1 PEB [15,16]. The ($\alpha\beta$) monomers are found as the basic building elements, they oligomerize face-to-face two ($\alpha\beta$) trimers in C₃ symmetry. The γ subunit is thought to be a hydrophobic linker protein and is situated in the central cavity of PE with a diameter of about 35 Å [17]. However its tertiary structure was not resolved due to rotational static disorder

Abbreviations: APC, allophycocyanin; B-PE, B-phycoerythrin; CD, circular dichroism; PBP, phycobiliprotein; PBsome, phycobilisome; PC, phycocyanin; PE, phycoerythrin; PEB, phycoerythrobin; PUB, phycourobilin; R-PE, R-phycoerythrin

^{*} Corresponding author. Tel.: +86 531 88364326; fax: +86 531 88564326.

E-mail address: zhangyz@sdu.edu.cn (Y.-Z. Zhang).

¹ These authors contributed equally to this work.

[15]. With such information, a static picture can be drawn of the 3D structure of PBP complexes under certain conditions. However, distinct protein environments may result in changes in protein–protein and pigment–protein interactions, as well as subsequent conformational variation. Therefore, the conformational flexibility of protein complexes *in vivo* may be a prerequisite for the physiological roles of proteins in response to environmental variations. For a better understanding of the protein conformation, crystallography information of the proteins of interest is thus required to be combined with active structural and functional investigations.

In this article, we explore the pH-induced conformational and functional dynamics of R-PE complexes in the range from 2 to 12. The spectroscopic and structural variations of R-PE monitored by means of absorption, fluorescence and circular dichroism (CD) spectra are investigated together with the analysis of the R-PE crystal structure. R-PE complexes from *P. urceolata* are shown to present structural flexibility and functional stability in response to environmental changes. Several key anchoring points are responsible for such an assembly conformation of the R-PE subunits. Active investigations of the structure and spectroscopy combined with analysis of the crystal structure of R-PE provide insights into its stability and the sensitivity of its conformations and functions.

2. Methods and materials

2.1. Sample preparation

The harvesting of *P. urceolata*, as well as the isolation and identification of R-PE, was carried out following the previously published protocol [18].

The pH adjustment was performed in solution containing 20 mM potassium phosphate buffer (pH 7.0) with HCl and NaOH modulating the solvent pH. Concentrated R-PEs were diluted with different pH solvents to a final concentration of 0.1 mg ml^{−1} and stirred for 5 min

Table 1

Sigmoidal fit parameters with different spectra of R-PE as a function of pH

Fit parameter	Acidic environment		Basic environment	
	x_0	p	x_0	p
A ₄₉₈	1.96 ± 0.274	5.17 ± 0.936	11.3 ± 0.0541	40.7 ± 6.02
A ₅₃₈	2.3 ± 0.126	6.81 ± 1.13	11.3 ± 0.0595	43.7 ± 7.83
A ₅₆₇	2.59 ± 0.0251	12.8 ± 1.75	11.3 ± 0.0553	49 ± 9.47
Ex ₅₆₅ Em ₅₇₈	2.96 ± 0.0536	10 ± 1.54	11 ± 0.0275	36.6 ± 2.79
Ex ₅₄₀ Em ₅₇₈	2.97 ± 0.0491	10 ± 1.41	11 ± 0.0275	36.8 ± 2.84
Ex ₄₉₈ Em ₅₇₈	3.05 ± 0.047	11 ± 1.59	11 ± 0.0282	36.4 ± 2.88
Em ₅₇₈ Ex ₅₆₇	2.94 ± 0.0443	9.03 ± 1.02	10.9 ± 0.0643	36.1 ± 6.59
Em ₅₇₈ Ex ₅₄₀	2.89 ± 0.0736	7.76 ± 1.23	10.8 ± 0.0663	35.2 ± 6.48
Em ₅₇₈ Ex ₄₉₈	2.89 ± 0.0752	7.95 ± 1.33	10.8 ± 0.0641	35.3 ± 6.33

before further measurements. For the refolding experiments, protein solutions at pH 2, 3, 11 or 12 were rapidly injected in corresponding NaOH or HCl stock buffers and quickly homogenized. No diluting effects were detected. For denaturation experiment, R-PEs were diluted to a final urea concentration of 8 M, and final R-PE concentration of 0.1 mg ml^{−1}.

2.2. Spectral measurement

Absorbance spectra were measured at room temperature by a UV/VIS-550 spectrophotometer (Jasco, Japan) at a protein concentration of 0.1 mg ml^{−1} using a 1 cm pathway quartz cell with a bandwidth of 2.0 nm. Room temperature fluorescence was recorded by a FP-6500 fluorescence spectrofluorometer (Jasco, Japan) at a protein concentration of 0.1 mg ml^{−1} with the proper excitation and emission wavelengths using a cell of 1 cm path length. UV and visible CD spectra of 0.1 mg ml^{−1} R-PE in various pH buffers were recorded at room temperature with a J-810 spectropolarimeter (Jasco, Japan) in cells of 1 cm path length. Secondary structures were calculated using the software provided by JACSO [19]. CD spectra in the visible range were smoothed by moving averaging. All spectra are from single of

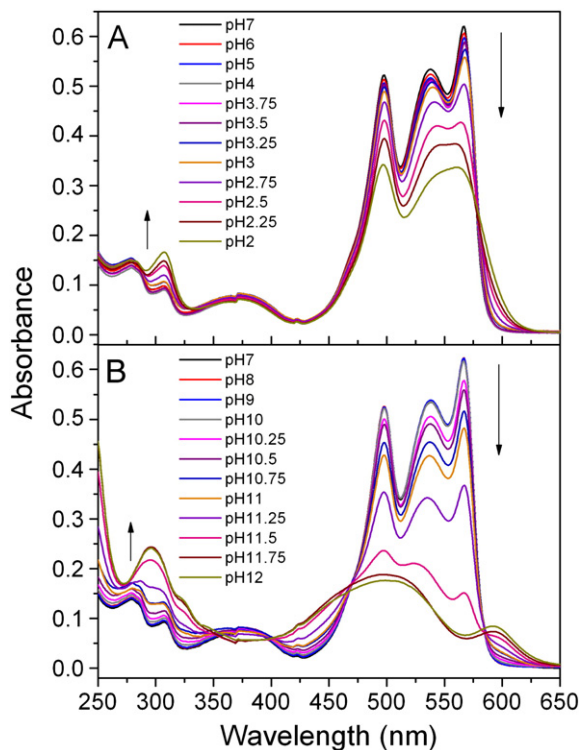


Fig. 1. Effects of solvent pH on the absorption spectra of R-PE in potassium phosphate buffer (20 mM). Spectra were recorded in a cell of 1 cm path length. The absorption maxima were at 498, 540, 565 nm. A, absorption spectra at pH 7–2; B, at pH 7–12.

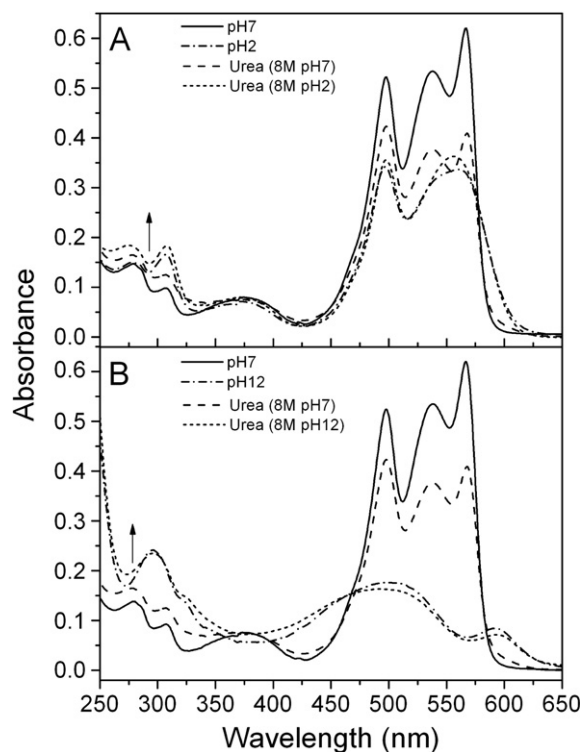


Fig. 2. Influence of urea (8 M) on the absorption spectra of R-PE at different pH. Absorption at neutral and acidic (pH 2) condition; absorption at neutral and basic (pH12) condition. Spectra of R-PE without urea are present as control.

repetitive experiments. Traces of peak intensities of absorbance and fluorescence spectra, as well as the fraction of secondary structures of R-PE, as a function of pH were fitted with a logistic function according to Kupka [13]: $y = A_2 + (A_1 - A_2) / (1 + (x/x_0)^p)$. Here x_0 is the inflection point, and p is the slope at x_0 . In an acidic environment, A_2 is the amplitude of native protein at neutral pH, and A_1 is the amplitude at pH 2. In a basic environment, A_1 is the amplitude of native protein at neutral pH, and A_2 is the amplitude at pH 12.

2.3. Structural analysis

Primary sequences of the α and β peptides of R-PE were analyzed from *P. urceolata* [16], *Gracilaria chilensis* [20] and *P. boldii* [21] using BioEdit (Ibis Biosciences). The structural analysis was performed based on the X-ray crystal structure of R-PE from *P. urceolata* (PDB code: 1lia) [15]. Structural analysis was performed using PyMol [22].

3. Results

3.1. Absorption spectra

Native R-PE in physiological conditions can strongly absorb light in the spectral region from 470 to 570 nm (Fig. 1). Successive reductions in the absorption of R-PE in an acidic environment are observed as the

solvent pH decreases (Fig. 1A), comprising faster decreases in the absorbances at 565 and 540 nm, which are attributed to PEB, and a relatively minor decline visible in the absorbance at 498 nm, corresponding to PUB due to a shorter conjugated π bond system [23]. The amplitudes of the absorption peaks at various pH values can be fitted with a sigmoidal function (Supplementary Fig. 1). According to the fit parameters summarized in Table 1, the absorbance at 565 nm decreases most dramatically, whereas the 498 nm peak decreases more slowly than the other two peaks in the visible range. The stronger stability of PUB is most likely due to the double binding of rings C and D in PUB to $\beta 50$ and $\beta 61$ Cys residues, respectively, whereas PEB is bound to the protein through only one Cys residue. Additionally, it may also be a consequence of the different extinction coefficients between native and denatured chromophores [24,25]. More significant decreases in absorbance are found when the pH is lower than 4. In addition to the rapid decline, below pH 3.0, the absorption maxima at 540 and 565 nm show a slight red- and blue-shift, respectively. At pH 2.25, these two absorption bands are fused into a broader band at intermediate wavelength. This may indicate that the local conditions of the PEB chromophores within R-PE are greatly affected. In addition, the absorption spectrum of R-PE in the visible range at pH 2 resembles that of denatured R-PE at the same pH (Fig. 2). In a basic solution, the absorption is fairly stable at pH 7–10 (Fig. 1B). At pH > 11, significant variations occur, including a rapid

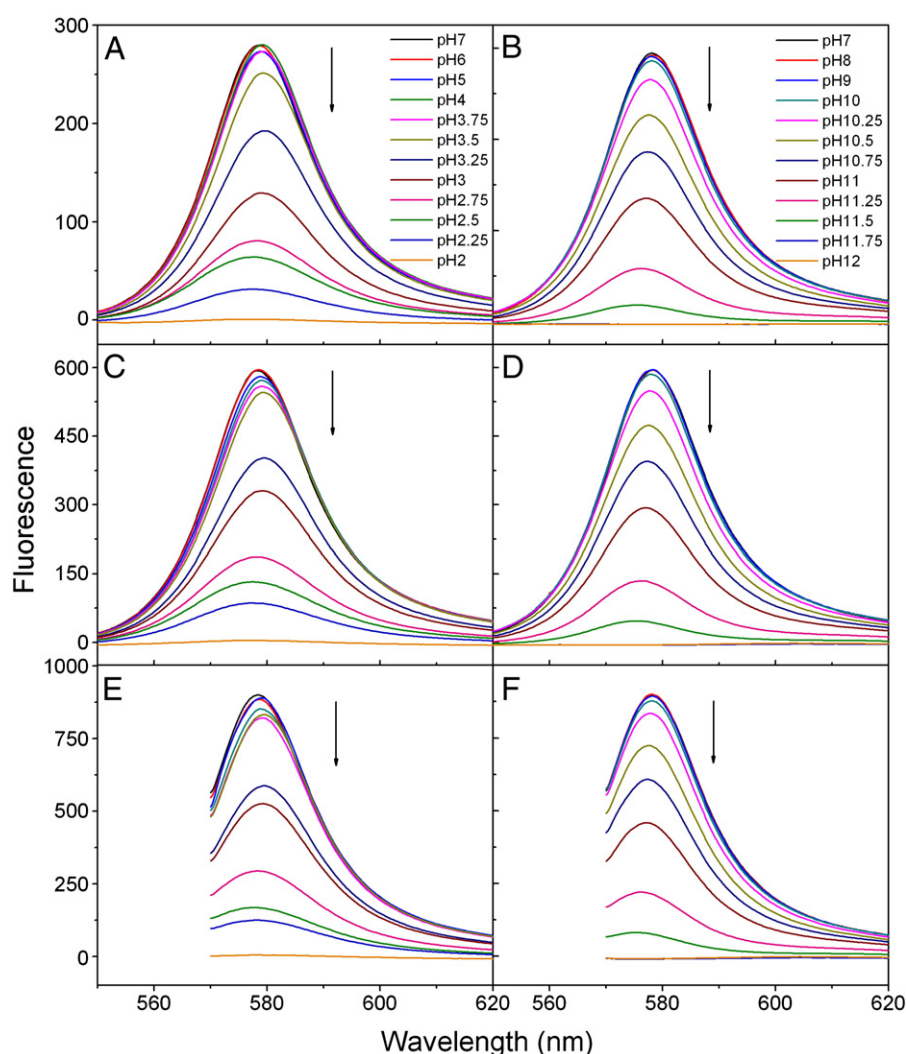


Fig. 3. Fluorescence emission spectra of R-PE (A, B excited at 498 nm; C, D excited at 540 nm; E, F excited at 565 nm) as a function of pH. The maximum of the fluorescence emission was at 578 nm. Fluorescence spectra of R-PE were measured in potassium phosphate buffer (20 mM) in a 1 cm length cell. A, C, E: Fluorescence emission spectra of R-PE at pH 7–2; B, D, F: at pH 7–12.

decrease in PEB absorption (A_{540} and A_{565}) and a remarkably broadened absorption at 498 nm. Interestingly, a rise in absorbance at 598 nm is observed. Differing from the red-shift observed in acidic solutions, A_{540} presents a blue-shift when the pH is modulated to a basic environment. We find that pH effects on R-PE absorption are more significant in basic conditions than in acidic conditions. This is consistent with the colors of R-PE solutions with different pH (data not shown).

Significant variations in the UV-absorption region also occur at $\text{pH} < 4$ and > 10 . When the pH is below 4 or above 10, A_{275} , arising from the aromatic amino acids, is slightly elevated. There is at the same time a significant increase in A_{310} , which is most likely the absorption of the chromophores [26]. Such observations may indicate conformational changes of the chromophores. At $\text{pH} > 11$, A_{310} and A_{275} fused to a broader band at 295 nm, accompanied by a shoulder at 325 nm, which might indicate a profound conformational change of the chromophores during the denaturation of R-PE. The pH induced irreversible changes may also be attributed to irreversible modifications of the chromophores.

For comparison, effects of full denaturation by urea (8 M) at neutral and extreme pH conditions are further studied (Fig. 2). We find that the urea-induced spectral change of R-PE in neutral condition, showing notable reduction of PEB and PUB absorbance, is not identical to those in extreme environments. In contrast, the spectral features of R-PE in extreme pH conditions ($\text{pH} 2$ and 12) with and without 8 M urea are more comparable. There is only a slightly reduced absorbance and blue-shift of the PEB band. The differences in fluorescence and CD spectra in the presence of urea are shown in Supplementary Figs. 2 and 3. This indicates that the interference of acidic and basic conditions is more pronounced

compared to the presence of the denaturant to induce the spectral variation of R-PE in extreme pH condition.

3.2. Fluorescence spectra

The changes of the fluorescence yield of R-PE in response to the pH perturbation are depicted in Fig. 3. The excitation at 498 nm, absorbed mostly by PUB, could be transferred to $\beta 84$ PEB, the terminal energy acceptor in R-PE, and generate fluorescence emission at 578 nm. When excited at 498 nm, the fluorescence emission at 578 nm decreases beyond the pH range of 3.5 to 10 (Fig. 3A and B). Fluorescence emission spectra with excitation at 540 and 565 nm may provide information about the energy transfer network between PEB chromophores. The decrease in the 578 nm emission implies the loss of fluorescence from $\beta 84$ PEB (Fig. 3C–F). More significant impacts are shown in basic conditions than in acidic solutions. Accompanied by the reduction in fluorescence emission at 578 nm, it is found that in an acidic environment, the fluorescence emission of R-PE exhibits a red-shift as pH is reduced; whereas in a basic environment, we find a blue-shift of fluorescence emission. They may also be caused by conformational changes or modifications of the chromophores.

We also examined the excitation spectra of R-PE solution with pH variations when the emission is at 578 nm (Supplementary Fig. 4). This showed relative stable spectra in the pH range of 3.5–10. Beyond this range, a faster decrease was observed. Furthermore, Supplementary Fig. 5 shows the normalized fluorescence drops similarly at all excitation wavelengths, indicating that the energy transfer is maintained even at extreme pH, whereas what is changing is probably the fluorescence yield of the emitting PEB chromophore(s). With variations in the pH conditions, conformational changes of protein

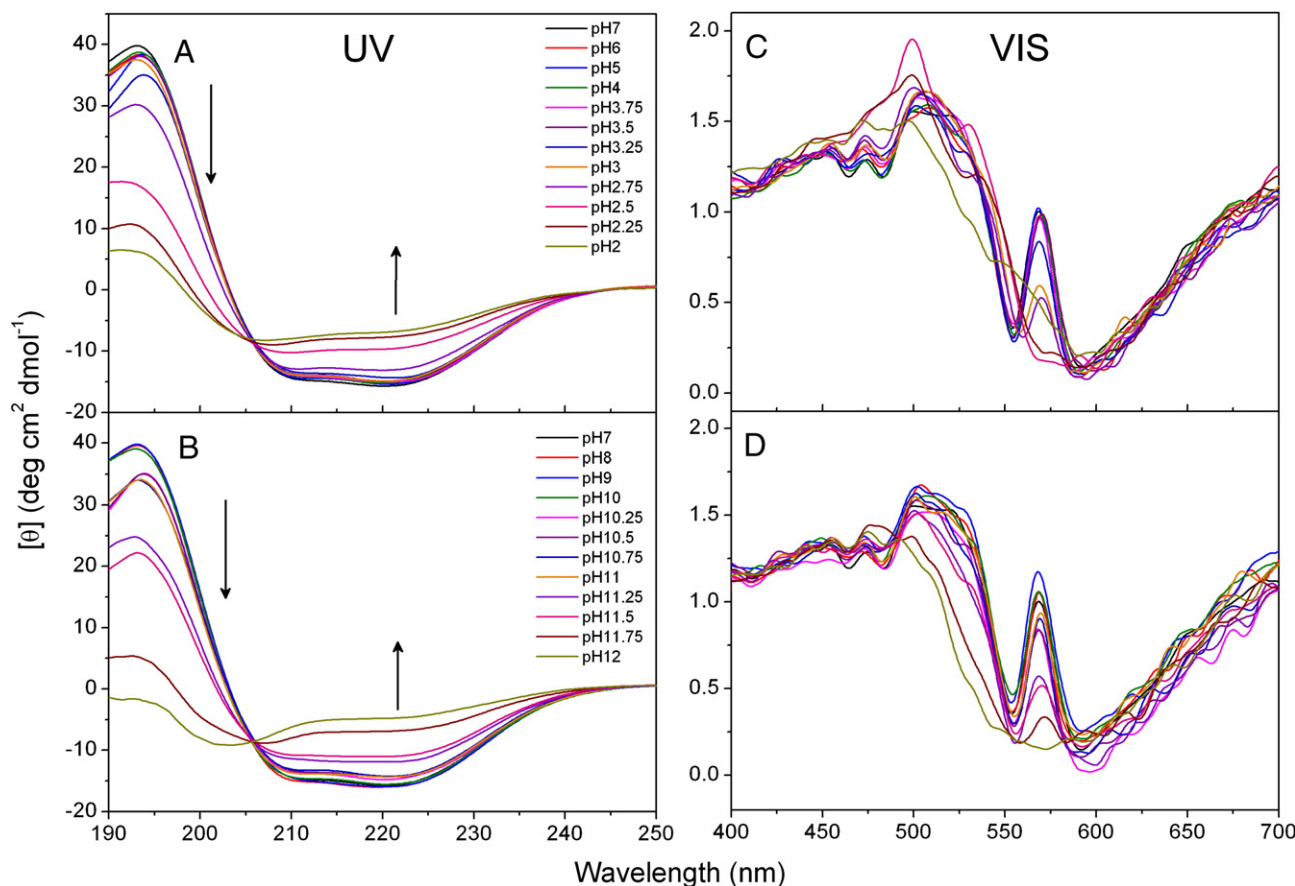


Fig. 4. Effects of solvent pH on CD spectra of R-PE. A, UV-CD spectra of R-PE at pH 7–2; B, UV-CD spectra of R-PE at pH 7–12; C, vis-CD spectra of R-PE at pH 7–2; D, vis-CD spectra of R-PE at pH 7–12. CD spectra of R-PE were measured in potassium phosphate buffer (20 mM) in a 1 cm length cell.

peptides and the local environmental altering of chromophores resulted in a sequential drop of fluorescence yield.

3.3. CD spectra

The spectral changes we observed may be an implication of the variation of R-PE structure in solvent environments, which can be monitored using CD spectra. Far-UV CD bands at 190–260 nm provide structural information regarding the peptide backbone and thus could be used to monitor conformational changes [27]. As depicted in Fig. 4A and B, when the α -helix structure dominates, CD spectra of R-PE show intense negative bands at 222 nm and 208 nm and a positive band located at 192 nm. They show that the characteristic CD peaks at 208 and 222 nm are both decreased and a reduction in the 192 nm CD signal is detected in acidic and basic solutions as compared to that at pH 7. In addition, a blue-shift in the negative CD band occurs as the solution becomes extremely acidic. A more apparent blue-shift is detected in basic conditions. This suggests that the secondary structure of R-PE is significantly altered by the pH variation.

The CD data were deconvoluted, and the results were fitted by a logistic function (Fig. 5 and Table 2). Secondary structure analysis showed that the amount of α -helix comprised up to 90% of the native structure. At pH 12, the α -helix content decreased to nearly zero but was maintained at 16% at pH 2. In the pH range of 3.5–10, most of the α -helix content was maintained, although there are some variations in α -helix content with respect to the pH changes.

The aggregation of the PBPs could be reflected in the visible region of the CD spectra. In the visible CD range (Fig. 4C and D), there are two positive peaks located at long wavelengths of 500 nm and 570 nm. The CD band at 570 nm shows a decrease when $\text{pH} < 3.5$ or > 10 , and a reduction in the CD peak at 500 nm is observed in basic conditions,

Table 2

Sigmoidal fit parameters with secondary structure fractions of R-PE as a function of pH

	Acidic environment		Basic environment	
	x_0	p	x_0	p
Helix	2.66 ± 0.0551	18.7 ± 6.03	12 ± 0.803	22.2 ± 8.5
Beta	2.65 ± 0.0412	17.9 ± 4.12	11.7 ± 0.266	36 ± 11.7
Random	2.7 ± 0.0329	20.8 ± 4.55	11.5 ± 0.18	32.6 ± 8.91

suggesting that there may be changes in the molecular structure or aggregation state within these pH ranges. However, there are no significant spectral changes in the pH range of 3.5–11, implying that the tertiary structure might be relatively stable at this pH range.

3.4. Refolding experiment

The electrostatic interactions and hydrogen bonds involved in the R-PE assembly are most likely affected by the pH-induced denaturation of the R-PE complex. There is a likelihood that these interactions could be reversibly recovered. To survey this, we adjusted the buffer pH from acidic (or basic) to a neutral status in order to study the refolding process of R-PE. On the basis of our observations, we tested four pH conditions: pH 2, 3, 11 and 12, where significant unfolding of R-PE occurs (Fig. 6). When the pH is altered back to 7 from both 3 and 11, the absorbance of R-PE tends to be recovered (Fig. 6). At pH 2, as mentioned earlier, A_{540} and A_{565} shift to become a broader absorbance, caused by the alteration in the micro-environment of the chromophores. After pH adjustment, the two individual absorptions are detected, but significant recovery of absorption ability is not visible (Fig. 6). This reveals that the absorbance capacity is only partially reversible under very violent denaturation. Similarly, when the pH condition is modulated back to neutral conditions from pH 12, the profile of the R-PE absorbance presents significant variations, mainly in the appearance of three typical R-PE absorption wavelengths, while the intensities seem irreversible due to the severe damage to the proteins solubilized in the extreme basic environment (Fig. 6). This may indicate that at pH 2 or 12, the structure of R-PE has been profoundly changed, which may seriously affect the refolding process, or the chromophores have been damaged.

Refolding of protein peptides and the assembly of R-PE subunits are also monitored by means of CD spectra (Supplementary Fig. 6). It is shown that influences on the secondary structures of R-PE subunits and the chromophore coupling are reversible at pH 3–11, but relatively irreversible unfolding of R-PE occurs at extreme conditions such as pH 2 and 12. With the adjustment of pH environment, visible CD spectra indicate the functional recovery of chromophores in R-PE. Far-UV CD data demonstrate that the local environment and coupling of adjacent chromophores can be altered in the pH range of 3 to 11, while less recovery is observed from more extreme conditions (pH 2 and 12) to neutral conditions. The close resemblance of the observations obtained from absorbance and CD spectra during R-PE refolding strongly indicates that the conformational change of R-PE may be a main cause of the spectroscopic variation with respect to pH alteration in the pH range 3–11.

4. Discussion

The use of biliproteins to study protein stability and unfolding has only partly been explored [12,13], although a wealth of information can principally be obtained due to the intrinsic probes, the covalently bound chromophores. Closer inspections of the absorbance, fluorescence and CD spectra allow us to better understand the pH-induced functional and conformational modulations of R-PE *in vitro*. Conformation of the protein can be evaluated from CD spectra, whereas the absorption and fluorescence spectra can indicate the functional changes.

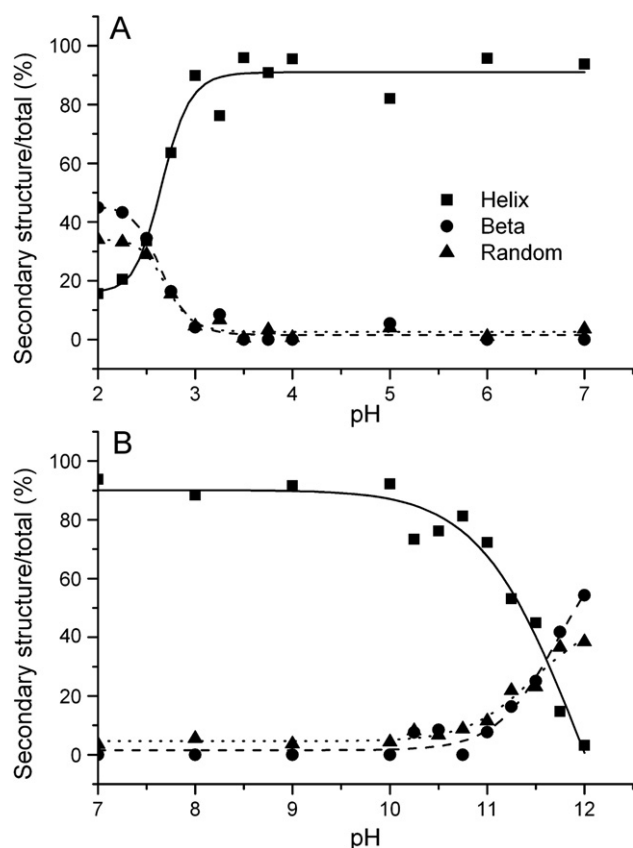


Fig. 5. Influence of pH on the secondary structure of R-PE. Fractions of α -helix (■, —), β structure (●, ·····), and random structure (▲, ---) are shown. Symbols are experimental values, and lines are the sigmoidal fits.

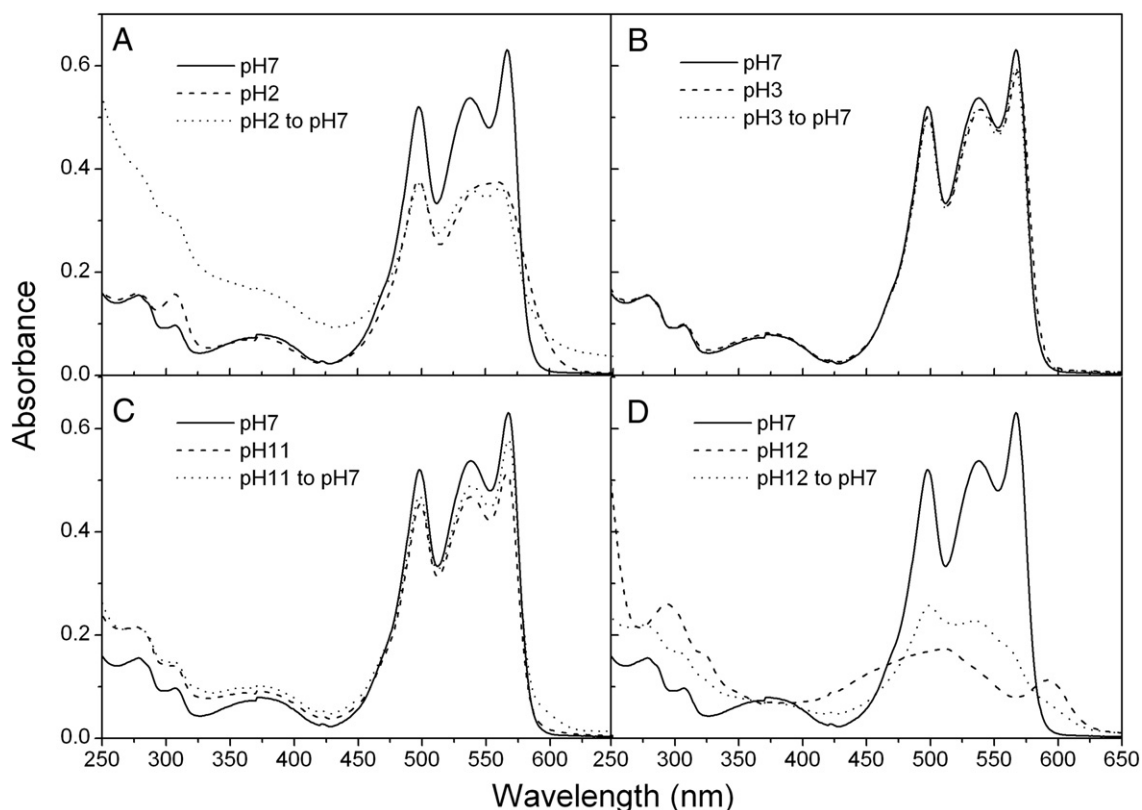


Fig. 6. Absorbance spectra of R-PE in protein refolding induced by pH adjustment. The solution pH was adjusted by rapidly injecting in corresponding NaOH or HCl stock buffers and quickly homogenized. A, pH 2–7; B, pH 3–7; C, pH 11–7; D, pH 12–7.

Changes in the solvent pH may result in the disturbance of electrostatic properties and hydrogen bonds involved in the protein association. During the pH-induced denaturation of R-PE, conformational variations of the chromophore–protein complexes allow the chromophores and local environment to be modified, giving rise to stronger exposure to solvent and changes in the distance between chromophores as well as between apoproteins and pigments. We have compared the spectra variation of R-PE in 8 M urea and in the absence of the denaturant at neutral and extreme pH (Fig. 2 and Supplementary Figs. 2, 3). Our data suggests that in addition to the denaturation, pH can also induce the changes of chromophore structure. The spectral shifts observed are most likely due to the transformation of chromophores caused by the protein-frame network movements. Moreover, the carboxylate groups of the protein involved in the stabilization of the conformation of the chromophores should be affected [23].

4.1. Stable function and flexible conformation of R-PE

The spectral changes in the pH range of 3.5 to 10 are very interesting. As depicted in Fig. 7, R-PE complexes present a broad range (pH 3.5 to 10) of absorbance and fluorescence stability. In this pH range, no remarkable changes in absorbance and fluorescence were observed, suggesting the stable energy transfer ability of the protein. In contrast, successive reduction in the intensity of CD spectra, which reflects the secondary structure, was detected. Deconvolution of the CD spectra revealed that the α -helix represents about 90% of the total secondary structure, which varies as the pH changes (Fig. 5). However, we noticed that in Fig. 5 the amount of secondary structure varies but does not change gradually as the CD data. After being fitted with a logistic function, the line between pH 3.5 and 10 seems to be flat. This may be a result from the deconvolution method. It should be mentioned that very low pH levels may cause denaturation of PBPs

including: i) dissociation of trimers to monomers, ii) dissociation of monomers into individual subunits, iii) (partial) unfolding of the subunits. However, in the pH range of 3.5–10, the aggregation state is maintained, as judged from the visible CD spectra.

This may suggest that the biological function of R-PE in this range is relatively independent of pH variation (absorption and fluorescence spectra), whereas its protein backbone is more sensitive with respect to environmental changes (CD spectra). Therefore, we propose that the fundamental tertiary structure of the R-PE molecule can be fixed by several specific anchoring positions in certain joint domains. Due to the rigid globin frame of R-PE, the local conditions of chromophores and some key amino acid residues (such as aromatic and charged amino acids), which are essential in the physiological roles of proteins, are more stable than other domains in the protein. In contrast, on the secondary structural level, flexible arrangements of the protein peptides are still allowed to a certain degree in response to environmental variations. This specific folding pattern may physiologically provide proteins with stable and adaptable spectroscopic properties under different environmental conditions.

4.2. R-PE in extreme pH

Beyond pH 3.5 and 10, pronounced spectral and structural changes occurred. The light absorption and energy transfer abilities of R-PE were both seriously affected, together with secondary structures. The harmful disturbance may break up the anchoring of R-PE, causing the significant loss of spectral properties and the drastic changes in the secondary structure of R-PE. It was elucidated that the carboxylates of Asp or Glu are close to the dissociation equilibrium, resulting in a rapid decrease in the absorbance and fluorescence [23]. In addition, we found that in extreme pH environments, the backbones formed a beta sheet structure, as revealed by the CD results, and their content may be more than 40%.

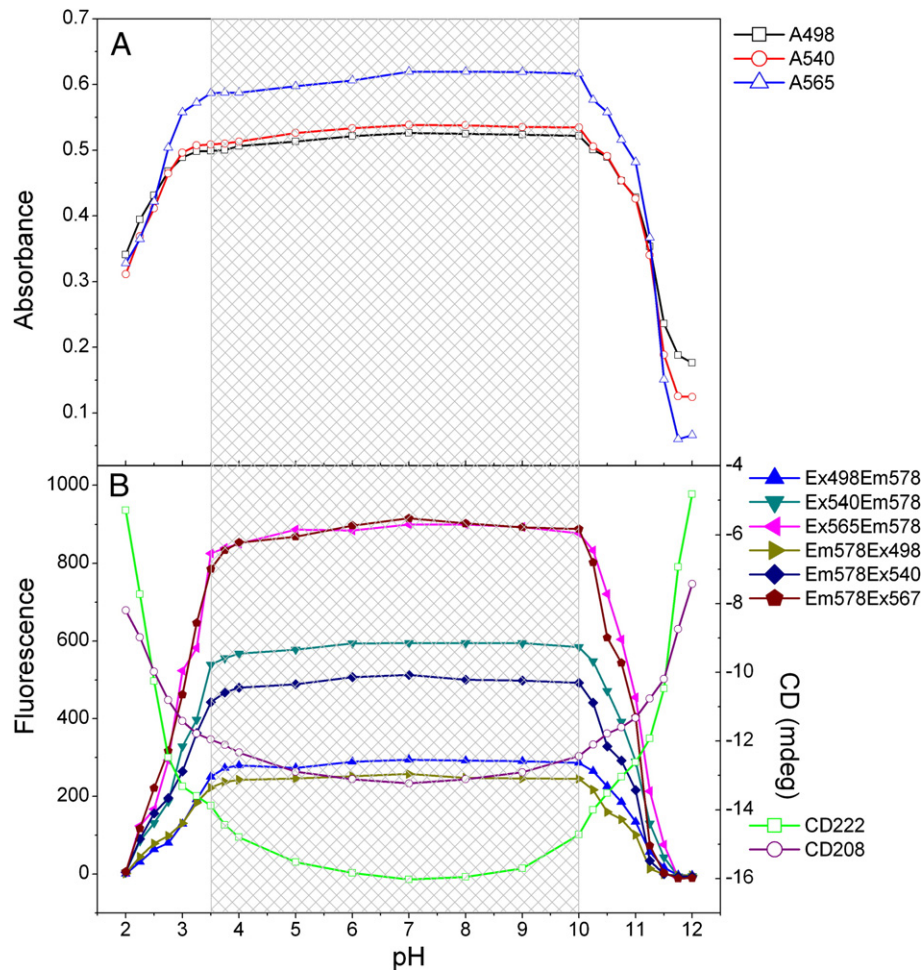


Fig. 7. Traces of peak intensities of absorbance, fluorescence and CD spectra of R-PE as a function of pH. Spectroscopic stability is shown in a broad range of pH representing by a sparse square.

We found in refolding experiments that, at pH 3 and 11, the structural and functional properties of proteins can still be greatly reversed. At very extreme conditions such as pH 2 and 12, the physiological properties are only partially reversible, due to the fact that the association of R-PE subunits dramatically collapses, and the peptides are largely exposed to the solvent or form a stable beta sheet structure, resulting in irreversible unfolding of R-PE.

4.3. Interaction surface of subunits

Crystal information of R-PE from *P. urceolata* (PDB code: 1lia) allows the interaction surface of individual subunits in R-PE to be analyzed (Supplementary Fig. 7). These anchoring positions and corresponding close contacts are clearly observed in three different

oligomerizations: ($\alpha\beta$) monomer, trimer and hexamer. By these polar contacts contributed by specific protein residues, the fundamental tertiary structure of the R-PE complex is stabilized, providing strong evidence for our proposed assembly model of R-PE proteins. The interactions between those specific residues on the anchoring surfaces of R-PE from *P. urceolata* are listed in Tables 3 and 4. Such results further reveal that the key anchoring points in the specific assembly of R-PE are highly correlated with the presence of charged amino acid residues. These protein residues are rich in α and β polypeptides: positively charged Arg residues (10 in α chain and 10 in β chain), negatively charged residues of Asp (9 in α chain and 11 in β chain) and Glu (10 in α chain and 7 in β chain). These three amino acid residues are frequently found in the key anchoring surfaces of R-PE, as depicted in Tables 3 and 4. Despite the stabilization effect, Asp residues are often observed in the proximity of the chromophores in R-PE, and they

Table 3
Polar contacts between α and β subunits in ($\alpha\beta$) monomer of R-PE

Residue	Chain	Amino acid	Residue	Chain	Amino acid	Distance (Å)
$\alpha 3$	A	Ser	$\beta 3$	B	Asp	3.16
$\alpha 10$	A	Ser	$\beta 110$	B	Arg	3.17
$\alpha 13$	A	Asp	$\beta 110$	B	Arg	2.92
$\alpha 13$	A	Asp	$\beta 94$	B	Tyr	2.65
$\alpha 13$	A	Asp	$\beta 93$	B	Arg	3.20
$\alpha 17$	A	Arg	$\beta 97$	B	Tyr	2.87
$\alpha 18$	A	Tyr	$\beta 89$	B	Glu	3.41
$\alpha 89$	A	Asp	$\beta 18$	B	Tyr	3.10
$\alpha 93$	A	Arg	$\beta 13$	B	Asp	2.74
$\alpha 96$	A	Asn	$\beta 19$	B	Val	2.89
$\alpha 97$	A	Tyr	$\beta 17$	B	Ala	2.70

Table 4
Polar contacts of ($\alpha\beta$) monomers in ($\alpha\beta$) trimer of R-PE

Residue	Chain	Amino acid	Residue	Chain	Amino acid	Distance (Å)
$\alpha 84$	A	PEB	$\alpha 77$	C	Thr	3.24
$\alpha 93$	A	Arg	$\alpha 76$	C	Tyr	2.74
$\alpha 110$	A	Trp	$\alpha 78$	C	Asn	3.46
$\alpha 119$	A	Tyr	$\alpha 78$	C	Asn	3.30
$\beta 76$	B	Tyr	$\alpha 93$	G	Arg	2.74
$\beta 77$	B	Thr	$\alpha 84$	G	PEB	3.24
$\beta 78$	B	Asn	$\alpha 110$	G	Trp	3.45
$\beta 78$	B	Asn	$\alpha 119$	G	Tyr	3.30

Chromophores involved in the interactions are highlighted.

were deduced to have a great influence in maintaining the lineal conformation of the chromophores [23,28]. All the chromophores in R-PE are hydrogen bonded to Asp residues. The carboxyl group of aspartic acid residues is protonated at the pH lower than the pKa of its side chain. Changes of pH condition in the low pH range will influence the stabilization of the conformation of each chromophore, as well as the spectra of R-PE. In addition, sequence alignment also shows that most of the key residues responsible for the anchoring are highly conserved, despite the fact that $\alpha 25$ Gln and $\alpha 18$ Tyr replace similar amino acids Glu and Phe, respectively (Supplementary Fig. 8). This may imply that the stabilization of homogenous tertiary structures of R-PE from different organisms is closely related to the interactions between these conserved anchoring residues.

Rich contents of aromatic amino acids were found in α and β peptide chains of R-PE from *P. urceolata*: Tyr (10 in α and 7 in β), Phe (3 in α and 3 in β) and Trp (1 in α). Structural analysis of the association of the R-PE complex also revealed that aromatic amino acids frequently locate at the key anchoring residues in the interaction surface and provide great contributions to the protein folding, such as $\alpha 18$ Phe and $\beta 18$ Tyr in monomer recognition, $\beta 74$ Tyr in trimer assembly as well as $\alpha 63$ Tyr and $\alpha 65$ Tyr in hexamer surface formation [23].

4.4. Implications to the physiological conformation of the PBP

The conformations of external light-harvesting proteins such as PE exposed to the cytoplasm or the plastid stroma may be affected by environmental changes. Thus, it is crucial for PE to maintain its functional stability with respect to certain conformational variations caused by environmental changes. Large transmembrane pH gradients are generated, for example, during the photosynthesis process. Changes in the environment, such as light intensity, can affect the linear electron flux, which is coupled with proton translocation [29]. It has been suggested that there are pH gradient changes at the photosynthetic membrane, responding to light changes [29]. However, R-PE *in vivo* may not encounter an extreme pH environment, but the conformational and functional changes may provide implications to the physiological dynamics of R-PE responses to the environment. Our results showed that, in spite of a certain extent of conformational variations of R-PE, most of the light-harvesting (revealed by the absorption spectra and fluorescence excitation spectra) and energy transfer (revealed by the fluorescence emission spectra) abilities are not considerably affected. This indicates that R-PE can retain the stability of its physiological function, while the protein backbones may show some conformational variations with respect to environmental changes. At the meantime, it should also be mentioned that while energy transfer within an R-PE unit is unaffected, the reduced fluorescence yield could result in a reduced energy transfer to neighboring PE or PC disks.

X-ray crystallographic structures of R-PE can provide precise and reliable information of protein conformation and interactions. However, to better understand the biological architectures and functions of proteins, active investigations are still required. Our work of combining static high-resolution X-ray pictures with the active biological functions of R-PE will provide new insights into the structure and function of light-harvesting proteins *in vivo*.

Acknowledgements

The work was supported by the National Natural Science Foundation of China (40676078, 40806056), Hi-Tech Research and Development Program of China (2008AA09Z404), Key International S&T Cooperation Project of China (2008DFA30440), Scientific and Technological Development Program of Shandong Province (2006CG2205009), and Foundation for Young Excellent Scientists in Shandong Province (2008BS02019).

Appendix A. Supplementary data

Supplementary data associated with this article can be found, in the online version, at doi:10.1016/j.bbabo.2009.02.018.

References

- [1] E. Gantt, Phycobilisomes, *Ann. Rev. Plant Physiol.* 32 (1981) 327–347.
- [2] A.N. Glazer, Phycobilisome. A macromolecular complex optimized for light energy transfer, *Biochim. Biophys. Acta* 768 (1984) 29–51.
- [3] A.N. Glazer, Light guides. Directional energy transfer in a photosynthetic antenna, *J. Biol. Chem.* 264 (1989) 1–4.
- [4] W.A. Sidler, Phycobilisome and phycobiliprotein structures, in: D.A. Bryant (Ed.), *The Molecular Biology of Cyanobacteria*, Kluwer Academic Publishers, Dordrecht, The Netherlands, 1994, pp. 139–216.
- [5] B.A. Zilinskas, L.S. Greenwald, Phycobilisome structure and function, *Photosynth. Res.* 10 (1986) 7–35.
- [6] N. Adir, Elucidation of the molecular structures of components of the phycobilisome: reconstructing a giant, *Photosynth. Res.* 85 (2005) 15–32.
- [7] L.N. Liu, X.L. Chen, Y.Z. Zhang, B.C. Zhou, Characterization, structure and function of linker polypeptides in phycobilisomes of cyanobacteria and red algae: an overview, *Biochim. Biophys. Acta* 1708 (2005) 133–142.
- [8] K.E. Apt, J.L. Collier, A.R. Grossman, Evolution of the phycobiliproteins, *J. Mol. Biol.* 248 (1995) 79–96.
- [9] A.N. Glazer, G.S. Apell, C.S. Hixson, D.A. Bryant, S. Rimon, D.M. Brown, Biliproteins of cyanobacteria and Rhodophyta: homologous family of photosynthetic accessory pigments, *Proc. Natl. Acad. Sci. U.S.A.* 73 (1976) 428–431.
- [10] S. Ritter, R.G. Hiller, P.M. Wrench, W. Welte, K. Diederichs, Crystal structure of a phycocouberin-containing phycoerythrin at 1.90-Å resolution, *J. Struct. Biol.* 126 (1999) 86–97.
- [11] C. Scharnagl, R. Raupp-Kossmann, S.F. Fischer, Molecular basis for pH sensitivity and proton transfer in green fluorescent protein: protonation and conformational substates from electrostatic calculations, *Biophys. J.* 77 (1999) 1839–1857.
- [12] Y. Ma, J. Xie, C. Zhang, J. Zhao, Three-stage refolding/unfolding of the dual-color b-subunit in R-phycoerythrin from *Polysiphonia urceolata*, *Biochem. Biophys. Res. Commun.* 352 (2007) 787–793.
- [13] M. Kupka, H. Scheer, Unfolding of C-phycoerythrin followed by loss of non-covalent chromophore–protein interactions 1. Equilibrium experiments, *Biochim. Biophys. Acta* 1777 (2008) 94–103.
- [14] W. Reuter, G. Wiegand, R. Huber, M.E. Than, Structural analysis at 2.2 Å of orthorhombic crystals presents the asymmetry of the allophycocyanin-linker complex, AP LC7.8, from phycobilisomes of *Mastigocladus laminosus*, *Proc. Natl. Acad. Sci. U.S.A.* 96 (1999) 1363–1368.
- [15] W.R. Chang, T. Jiang, Z.L. Wan, J.P. Zhang, Z.X. Yang, D.C. Liang, Crystal structure of R-phycoerythrin from *Polysiphonia urceolata* at 2.8 Å resolution, *J. Mol. Biol.* 262 (1996) 721–731.
- [16] T. Jiang, J.P. Zhang, D.C. Liang, Structure and function of chromophores in R-phycoerythrin at 1.9 Å resolution, *Proteins* 34 (1999) 224–231.
- [17] R. Ficner, R. Huber, Refined crystal structure of phycoerythrin from *Porphyridium cruentum* at 0.23-nm resolution and localization of the gamma subunit, *Eur. J. Biochem.* 218 (1993) 103–106.
- [18] L.N. Liu, X.L. Chen, X.Y. Zhang, Y.Z. Zhang, B.C. Zhou, One-step chromatography method for efficient separation and purification of R-phycoerythrin from *Polysiphonia urceolata*, *J. Biotechnol.* 116 (2005) 91–100.
- [19] J.T. Yang, C.S. Wu, H.M. Martinez, Calculation of protein conformation from circular dichroism, *Methods Enzymol.* 130 (1986) 208–269.
- [20] C. Contreras-Martel, J. Martinez-Oyanedel, M. Bunster, P. Legrand, C. Piras, X. Verne, J.C. Fontecilla-Camps, Crystallization and 2.2 Å resolution structure of R-phycoerythrin from *Gracilaria chilensis*: a case of perfect hemihedral twinning, *Acta Crystallogr. D Biol. Crystallogr.* 57 (2001) 52–60.
- [21] M.K. Roell, D.E. Morse, Organization, expression and nucleotide sequence of the operon encoding R-phycoerythrin alpha and beta subunits from the red alga *Polysiphonia boldii*, *Plant Mol. Biol.* 21 (1993) 47–58.
- [22] W.L. DeLano, The PyMOL Molecular Graphics System. <http://www.pymol.org>, (2002).
- [23] J. Martinez-Oyanedel, C. Contreras-Martel, C. Bruna, M. Bunster, Structural-functional analysis of the oligomeric protein R-phycoerythrin, *Biol. Res.* 37 (2004) 733–745.
- [24] A.N. Glazer, C.S. Hixson, Characterization of R-phycoerythrin. Chromophore content of R-phycoerythrin and C-phycoerythrin, *J. Biol. Chem.* 250 (1975) 5487–5495.
- [25] A.N. Glazer, C.S. Hixson, Subunit structure and chromophore composition of rhodophytan phycoerythrins. *Porphyridium cruentum* B-phycoerythrin and b-phycoerythrin, *J. Biol. Chem.* 252 (1977) 32–42.
- [26] P. ÓCarra, C. ÓEocha, D.M. Carroll, Spectral properties of the phycobilins II. Phycoerythrobilin, *Biochemistry* 3 (1964) 1343–1350.
- [27] N.J. Greenfield, Circular dichroism analysis for protein–protein interactions, *Methods Mol. Biol.* 261 (2004) 55–78.
- [28] H. Kikuchi, H. Wako, K. Yura, M. Go, M. Mimuro, Significance of a two-domain structure in subunits of phycobiliproteins revealed by the normal mode analysis, *Biophys. J.* 79 (2000) 1587–1600.
- [29] D.M. Kramer, T.J. Avenson, G.E. Edwards, Dynamic flexibility in the light reactions of photosynthesis governed by both electron and proton transfer reactions, *Trends Plant Sci.* 9 (2004) 349–357.